



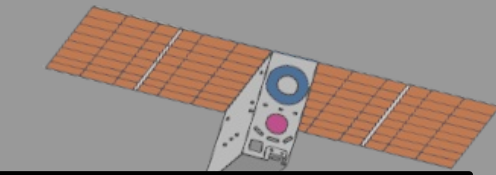
# DIDYMOS AND DIMORPHOS SURFACE AND EJECTA REFLECTANCE PROPERTIES THROUGH DART AND LICIAcube IMAGING

**Pedro Henrique Hasselmann<sup>1</sup>, E. Dotto<sup>(1)</sup>, J.D.P. Deshapriya<sup>(1)</sup>, G. Poggiali<sup>(2,3)</sup>, A. Rossi<sup>(4)</sup>, I. Bertini<sup>(5)</sup>, G. Zanotti<sup>(6)</sup>, S. Ieva<sup>(1)</sup>, S. Ivanovski<sup>(7)</sup>, E. Mazzotta-Epifani<sup>(1)</sup>, V. Della Corte<sup>(8)</sup>, J. Sunshine<sup>(9)</sup>, A. Zinzi<sup>(10,11)</sup>, J-Y. Li<sup>(12)</sup>, L. Kolokolova<sup>(13)</sup>, D. Glenar<sup>(14,15,16)</sup>, R. Lolachi<sup>(14,15,16)</sup>, T. Stubbs<sup>(15)</sup>, M. Amoroso<sup>(11)</sup>, O. Barnouin<sup>(17)</sup>, J.R. Brucato<sup>(2)</sup>, N. Chabot<sup>(17)</sup>, A. Cheng<sup>(17)</sup>, A. Capannolo<sup>(18)</sup>, S. Caporali<sup>(1)</sup>, M. Ceresoli<sup>(6)</sup>, B. Cotugno<sup>(19)</sup>, G. Cremonese<sup>(20)</sup>, T. R. Daly<sup>(17)</sup>, M. Dall’Ora<sup>(21)</sup>, V. Di Tana<sup>(19)</sup>, C.M. Ernst<sup>(17)</sup>, E.G. Farnham<sup>(9)</sup>, F. Ferrari<sup>(6)</sup>, I. Gai<sup>(22)</sup>, G. Impresario<sup>(10)</sup>, D. P. Sanchez-Lana<sup>(23)</sup>, M. Lavagna<sup>(6)</sup>, A. Lucchetti<sup>(20)</sup>, F. Miglioretti<sup>(19)</sup>, D. Modenini<sup>(22)</sup>, M. Pajola<sup>(20)</sup>, S. Pirrotta<sup>(10)</sup>, P. Palumbo<sup>(5)</sup>, D. Perna<sup>(1)</sup>, S.D. Raducan<sup>(24)</sup>, A. Rivkin<sup>(17)</sup>, S.R. Schwartz<sup>(12)</sup>, S. Simonetti<sup>(19)</sup>, P. Tortora<sup>(22)</sup>, J.M. Trigo-Rodríguez<sup>(26)</sup>, M. Zannoni<sup>(22)</sup>.**

1-INAF-Osservatorio Astronomico di Roma, Monte Porzio Catone, Roma, Italy; 2-INAF-Osservatorio Astrofisico di Arcetri, Firenze, Italy; 3-LESIA-Observatoire de Paris PSL, Paris, France; 4-IFAC-CNR, Sesto Fiorentino, Firenze, Italy; 5-Università degli Studi di Napoli “Parthenope”, Dip. di Scienze & Tecnologie, Centro Direzionale, Napoli, Italy; 6-Politecnico di Milano, Dip. di Scienze e Tecnologie Aerospaziali, Milano, Italy; 7-INAF-Osservatorio Astronomico di Trieste, Trieste, Italy; 8-INAF-Istituto di Astrofisica e Planetologia Spaziali, Roma, Italy; 9-University of Maryland, Department of Astronomy, MD-USA; 10-Agenzia Spaziale Italiana, Roma, Italy; 11-Space Science Data Center – ASI, Roma Italy; 12-Planetary Science Institute, University of Arizona, Tucson, AZ-USA; 13-University of Maryland, College Park, MD-USA; 14-University of Maryland, Baltimore Co., Baltimore, MD-USA; 15-NASA Goddard Space Flight Center, Greenbelt, MD-USA; 16-Center for Research and Exploration in Space Science and Technology, NASA/GSFC, Greenbelt, MD-USA; 17-Johns Hopkins University Applied Physics Laboratory, Laurel, MD-USA; 18-ISAE-SUPAERO, Université de Toulouse, Toulouse, France; 19-Argotec, Torino, Italy; 20-INAF- Osservatorio Astronomico di Padova, Padova, Italy; 21-INAF-Osservatorio Astronomico di Capodimonte, Napoli, Italy; 22-Università di Bologna, Dip. di Ingegneria Industriale, Forlì, Italy; 23-CCAR, The University of Colorado, Boulder, CO-USA; 24-University of Bern, Bern, Switzerland; 25-Jet Propulsion Laboratory, California Institute of Technology, Pasadena, CA-USA; 26-Institute of Space Sciences (CSIC), Barcelona, Spain.

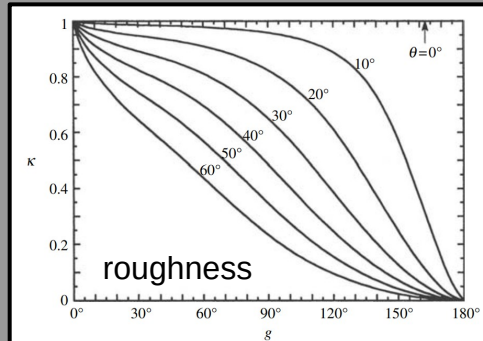
**Corresponding author :** [pedro.hasselmann@inaf.it](mailto:pedro.hasselmann@inaf.it)

# Albedo and phase curve studies, why?

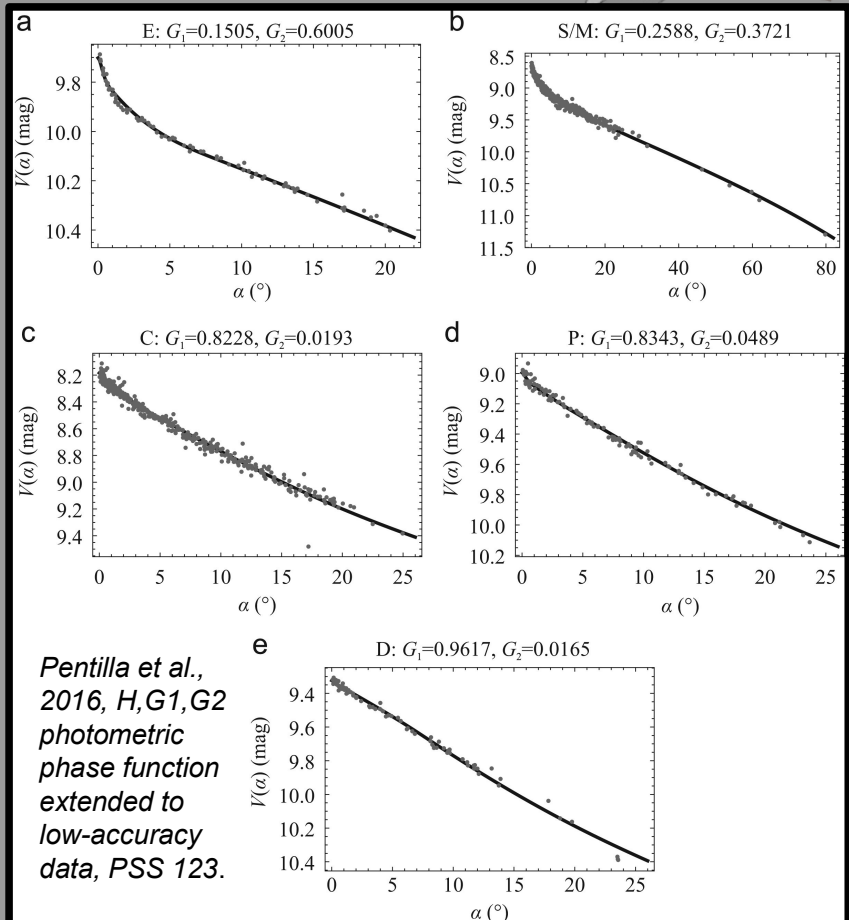


Asteroid photometric phase curves are a collective expression of the light reflection scattering from atmosphereless granular medium with large grain size range and topographically complex.

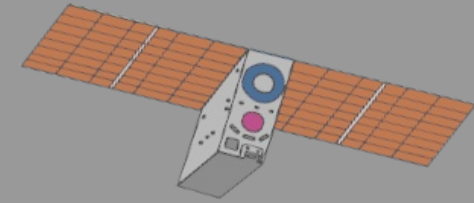
The morphology of integrated phase curves are tools for reinforcing our understanding on the asteroid composition ( $0^\circ < \alpha < 40^\circ$ , Pentilla et al., 2016; Belskaya & Shevchenko, 2000) and surface structures ( $\alpha > \sim 40^\circ$ , packing, shadowing-roughness, Hapke, 2012,).



Hapke, 2012, Cambridge Book, 2nd. Ed.

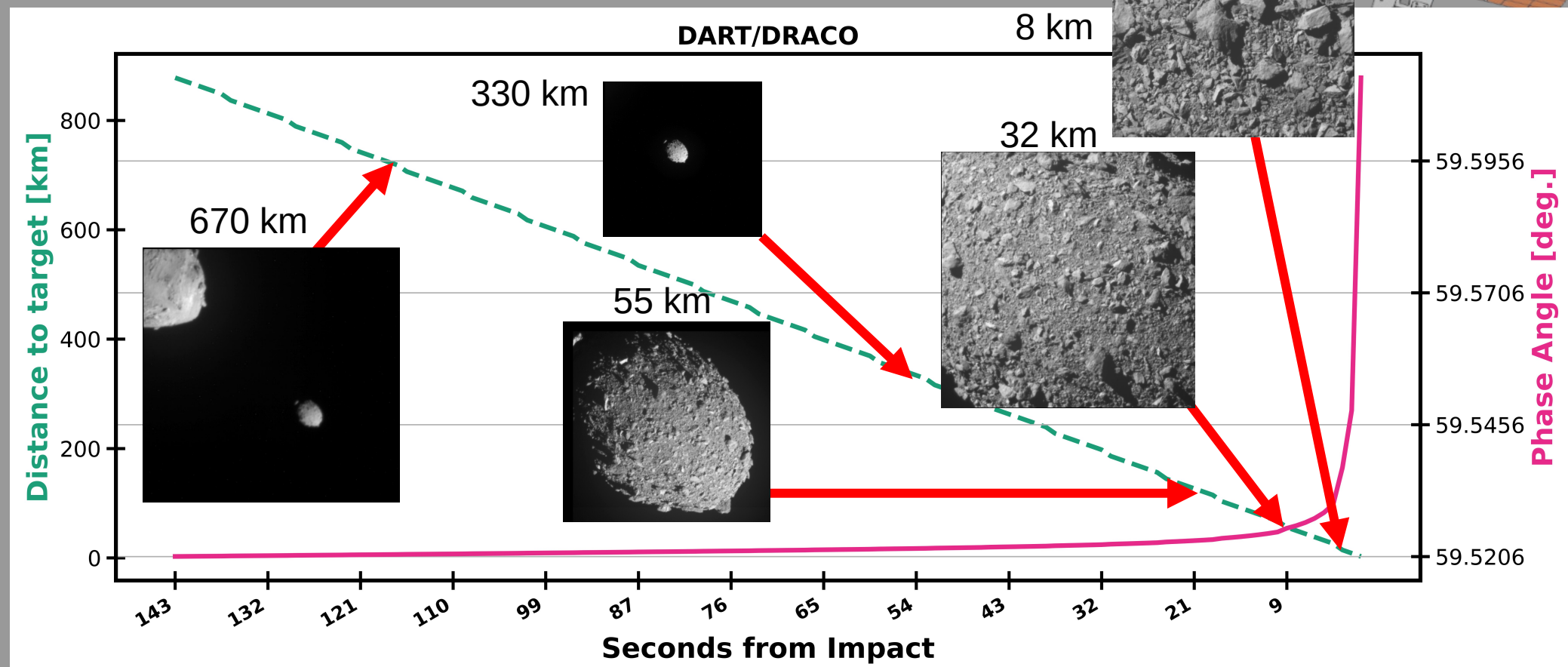


# *What are our goals here?*

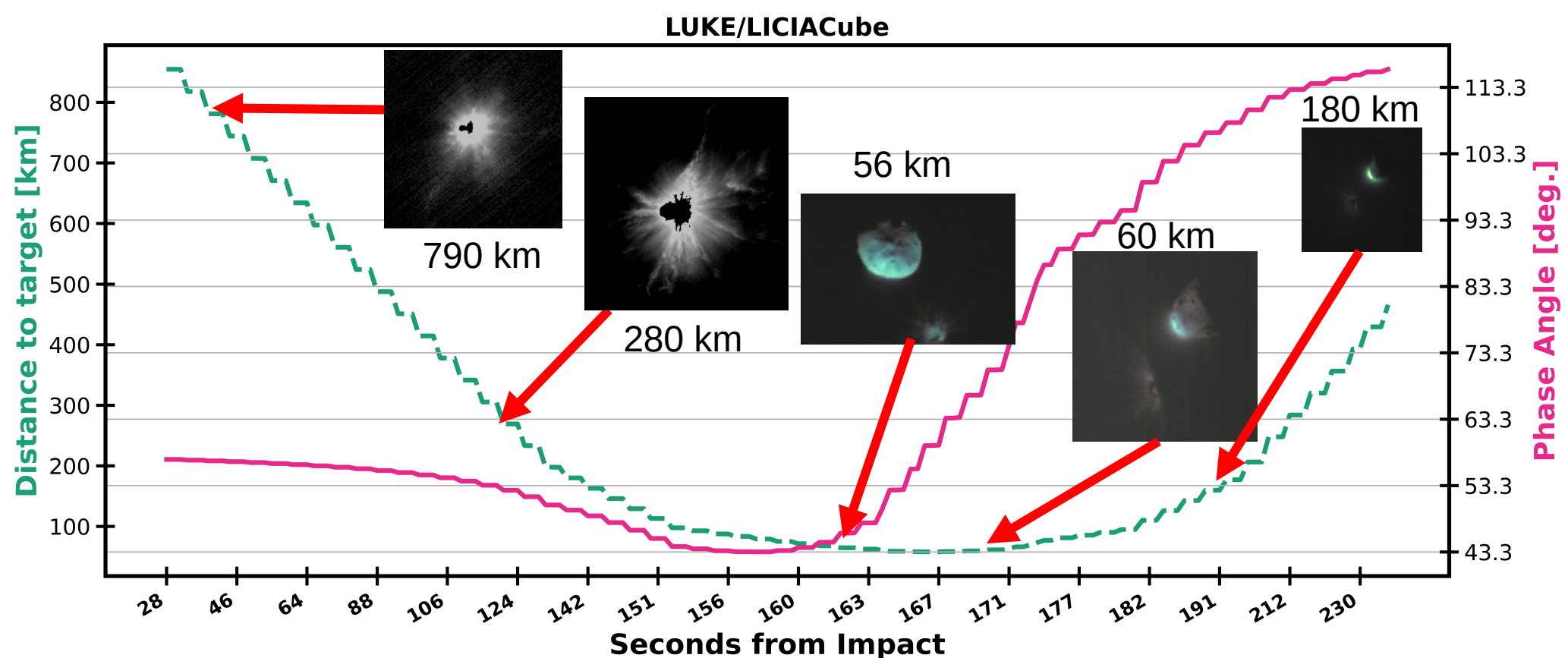
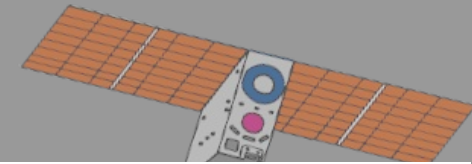


- Cast a bit of light into the composition nature of Didymos and Dimorphos.
- Check whether Didymos and Dimorphos have similar composition or surface properties given their phase curve and reflectance distribution function.
- On what Hapke and HG1G2 parameters can tell us as comparative tool to other asteroids and surfaces.
- And what are the most likely compositional scenarios.

# DART/DRACO Images (before impact)



# LICIACube/LUKE Images (after)

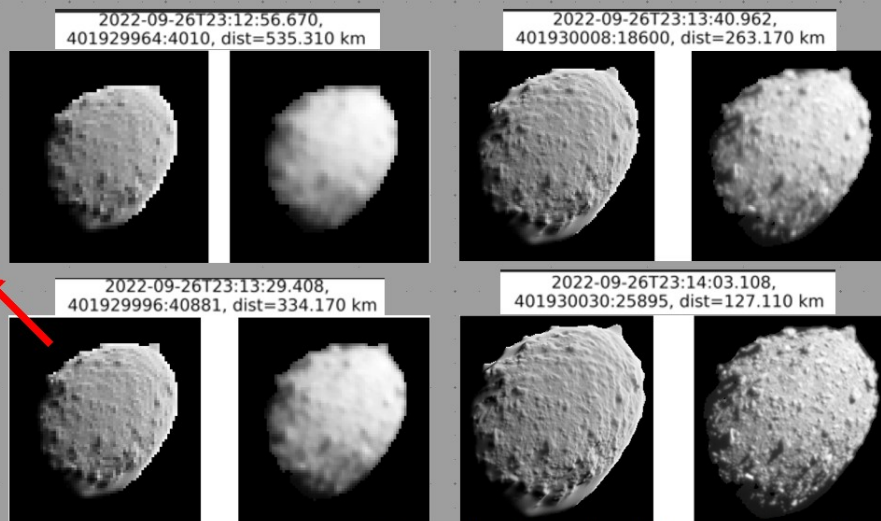


# DRACO's Disk-resolved Dimorphos

Update from AGU 2022:

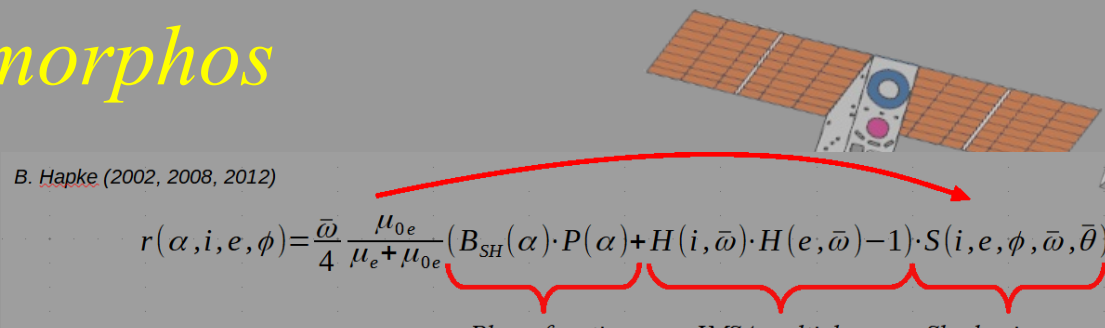
16 selected radiometric-calibrated images during approach from <60 km to Dimorphos (new backplanes).

Preliminary Hapke Analysis indicates an overall parameters more akin to Lutetia (M-type,  $\rho_v=0.19$ ), and Ida (S-Type,  $\rho_v=0.20$ ) (Hasselmann et al., 2016; Sato et al., 2014; Helfenstein et al., 1996).



Dimorphos' North Pole

Example of Synthetic Image Matching  
Using Shapeimager (Hasselmann et al., 2020, Icarus)



B. Hapke (2002, 2008, 2012)

$$r(\alpha, i, e, \phi) = \frac{\bar{\omega}}{4} \frac{\mu_{0e}}{\mu_e + \mu_{0e}} (B_{SH}(\alpha) \cdot P(\alpha) + H(i, \bar{\omega}) \cdot H(e, \bar{\omega}) - 1) \cdot S(i, e, \phi, \bar{\omega}, \bar{\theta})$$

Phase function      IMSA multiple-scattering      Shadowing-Roughness

$$r(\alpha, i, e, \phi) = \frac{1}{4} \bar{\omega} (P + M(i, e, \bar{\omega})) \cdot S'(i, e, \phi, \bar{\omega}, \bar{\theta})$$

Free Variables :

$\omega$  → average single-scattering albedo

$\theta$  → average roughness slope

$P$  → phase function at  $\alpha$

Prelim. Hapke IMSA parameters using Variational Bayesian Inference (Kingma & Welling, 2014, AVBS):

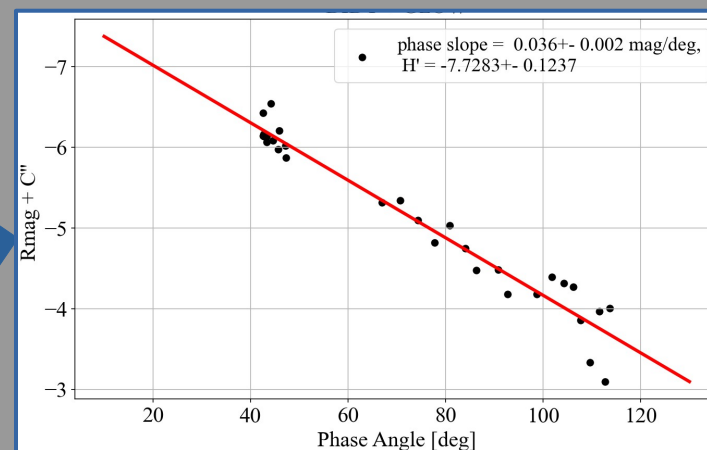
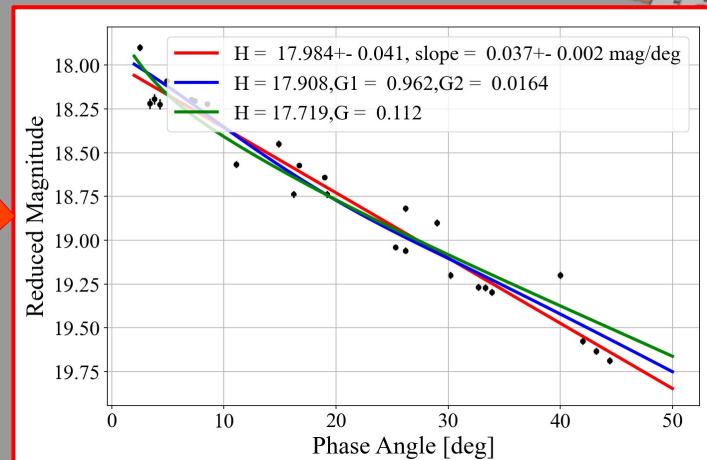
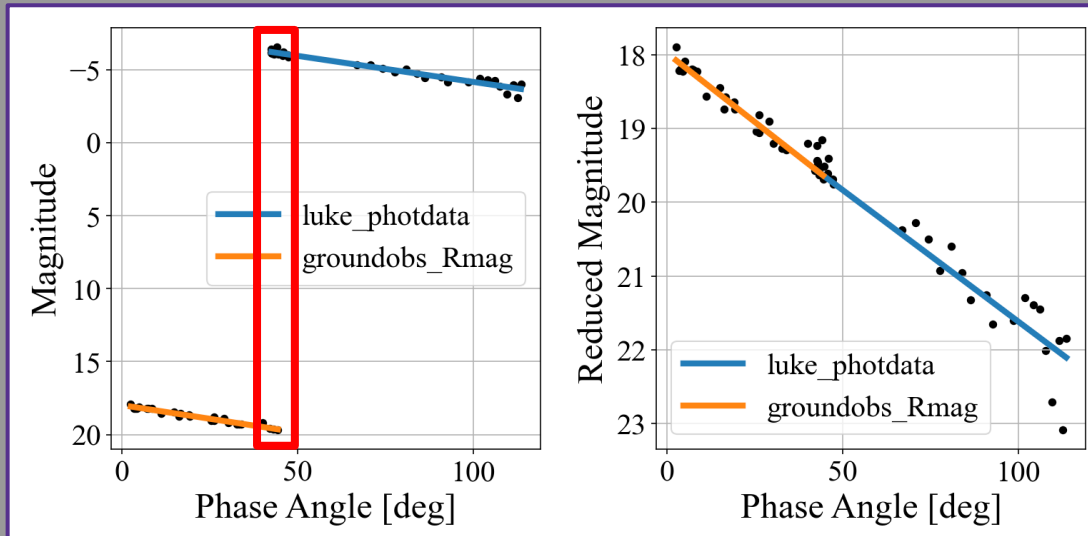
	This work	Lutetia	Ida	S-type
w	0.21+-0.02	0.22	0.22	0.39
P(59°)	2.20+-0.15	1.4	1.4	1.3
θ	25°+-4°	29°	20°	30°

# Ground Observations + LUKE



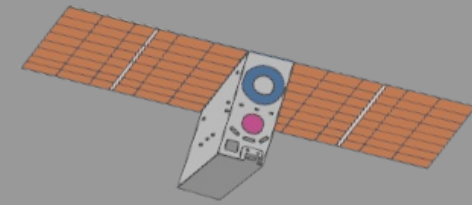
Ground-Obs and LUKE display similar phase slope.

Multi-Epoch Photometry → Pravec et al., (2006, 2022), private comm.

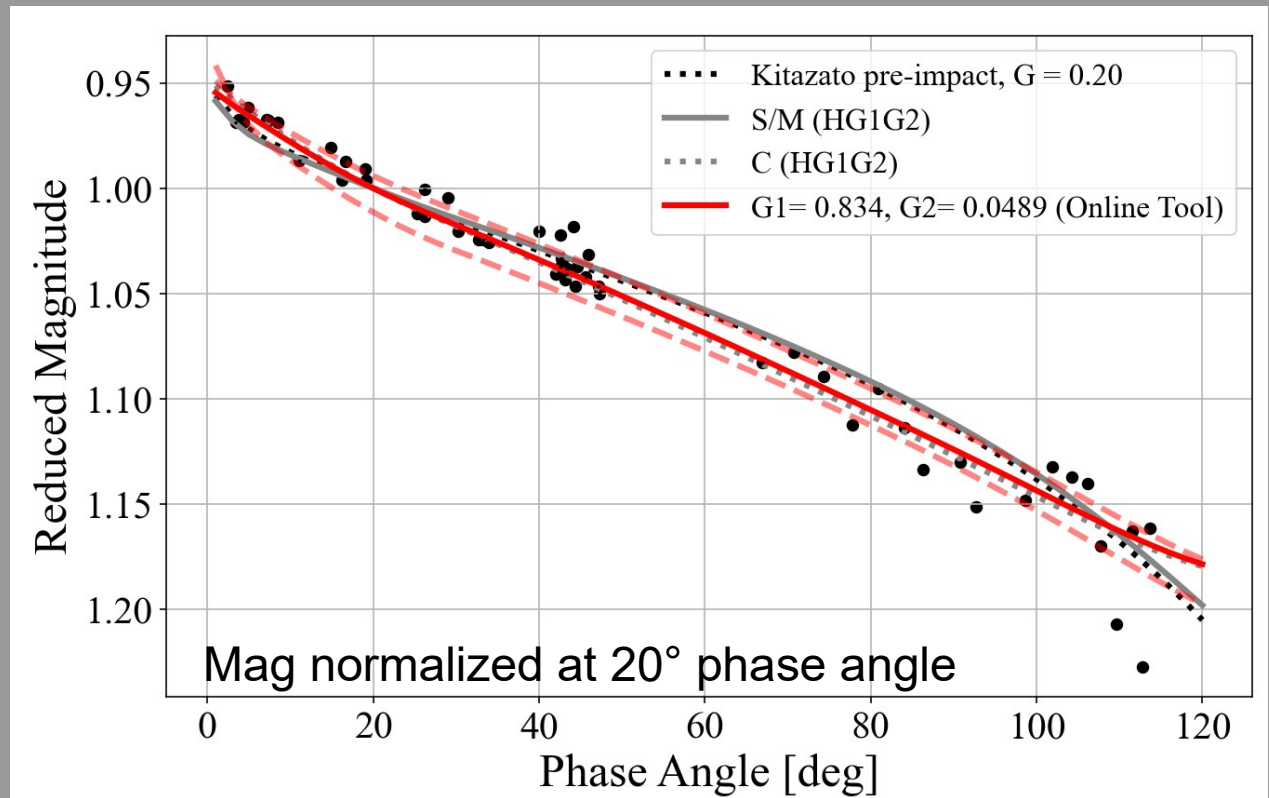


Preliminary reduced magnitude calibration was done using superimposed points at  $\sim 40^\circ$ .

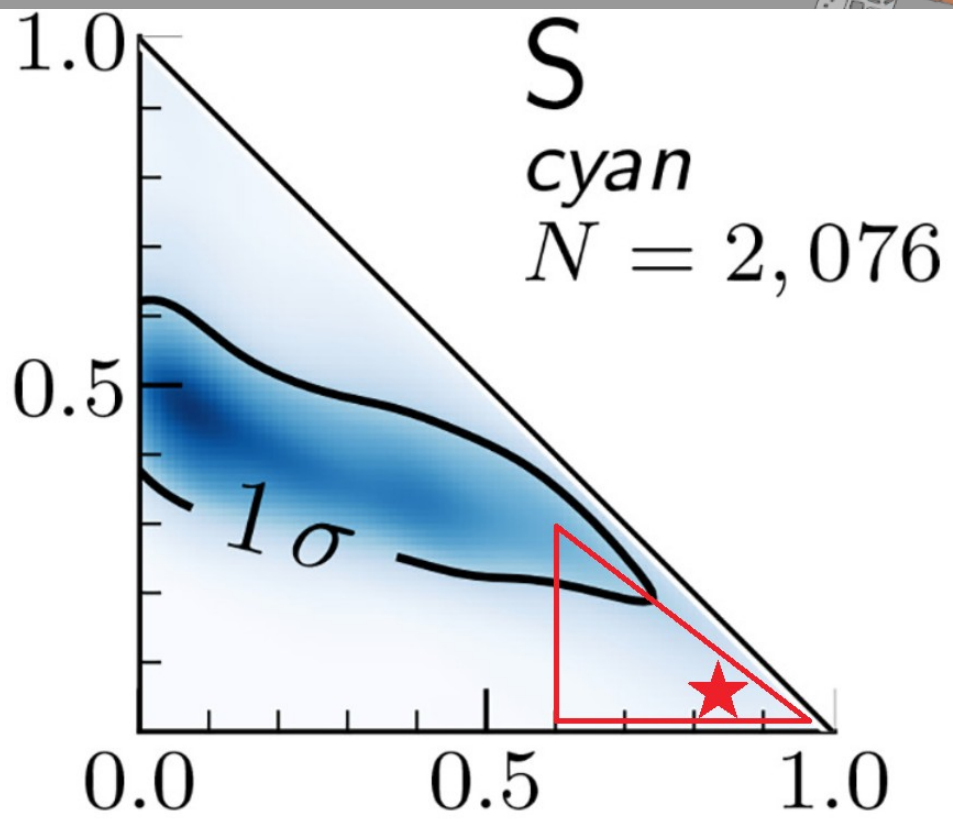
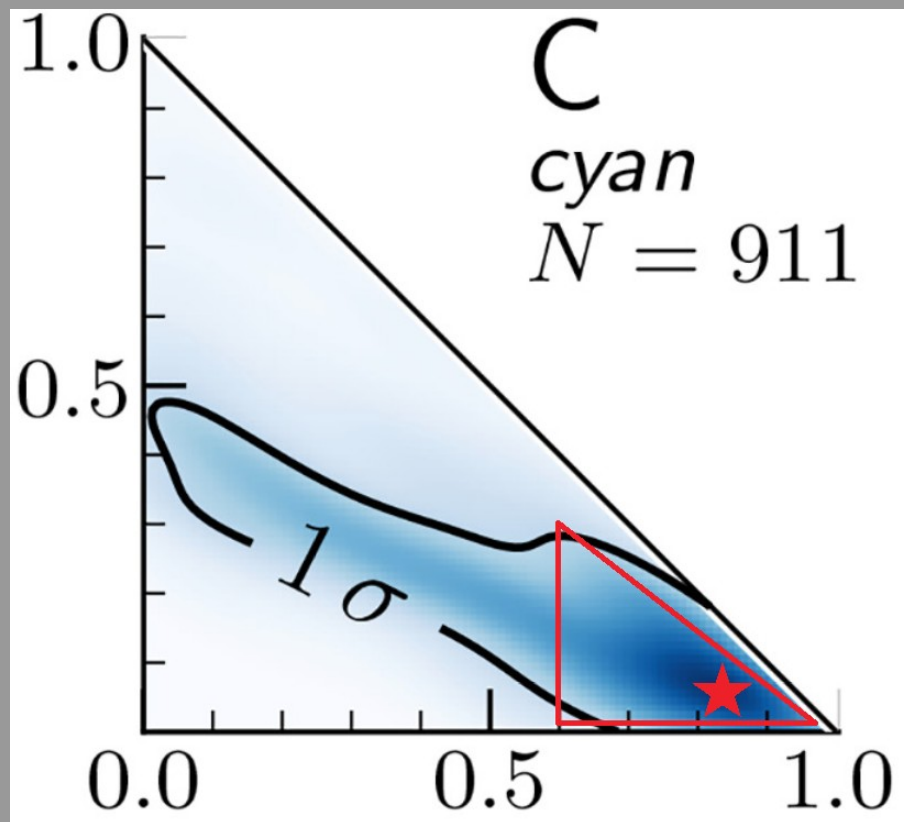
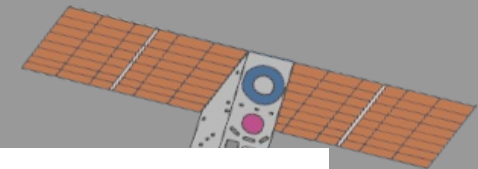
# *LUKE's Didymos Integrated Phase Curve*



- LUKE Calibrated (actual state, on-going).
- 34 R-plane short-exposure (<5 ms) images of non-saturated Didymos. Integrated over all signal under illuminated surface.
- R-bayer → R-cousin (Park et al., 2016, Adv.Sp.Res)
- Ejecta signal is under noise at the projected distance to Didymos.
- Full target cross-section computed through Synthetic Imaging using Didymos Shape Model and SPICE Kernels (DRACO & LICIAcube Team).
- Pre-impact H,G reference: Kitazato et al., 2004, LPSC. **Phase angle < 40°**.



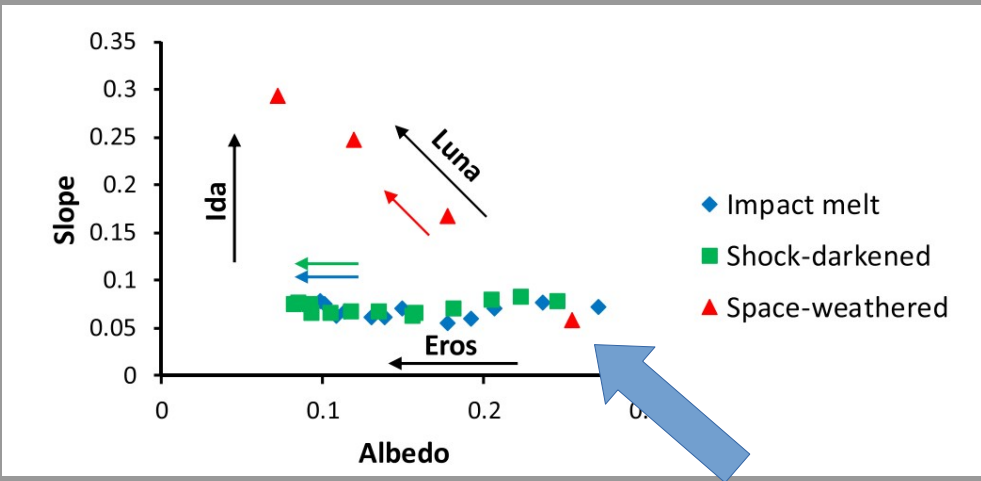
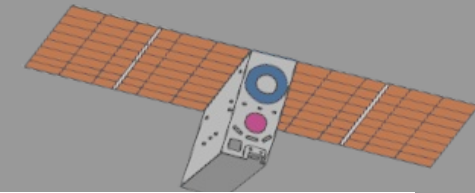
C, S/M HG1G2: Pentilla et al., 2016, PSS 123.



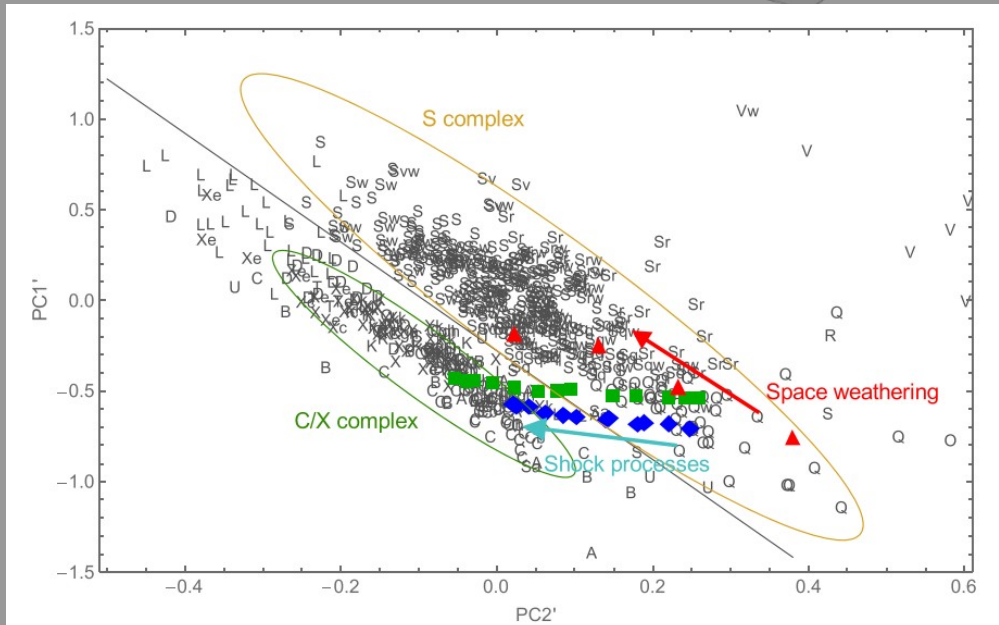
Solution → Pentilla's Online Tool  
Std. Dev. → 30 tests with Basin-hopping algorithm

Makhler et al., 2021, Icarus 354

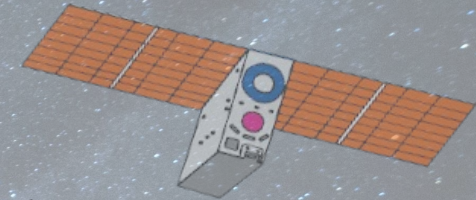
# Shock-Darkening/Impact melts?



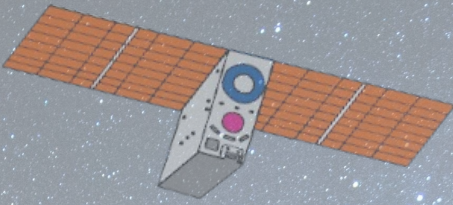
*Variegation detection  
with LUKE  
can help here!*



# The take away



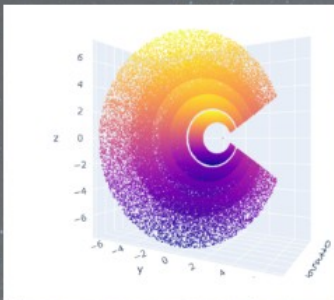
- LICIACube provides essential data to complete the phase curves into larger phase angles. Generally inaccessible from ground-observations. DRACO disk-resolved images provide enough anchor points to estimate some of the Hapke parameters.
- Didymos phase curve and Dimorphos Hapke parameters to point to objects with surface properties of possibly similar composition.
- Didymos phase curve and Dimorphos BRDF seems to point to objects with surface properties at the dark-end of S-types. **Didymos  $\rho_v$  is estimated to 0.15 (S-type  $\rho_v=0.22$ )**. *S-type mixed with carbonaceous materials or shock-darkening? Other examples in the NEOs phase curve's literature (1998 OR2, Battle et al., 2022)?*
- Dimorphos' phase curve from LICIACube will require disentangling it from the ejecta's contribution and/or using only post-closest approach “back-view” images (larger phase angles) – ***On-going analysis***.



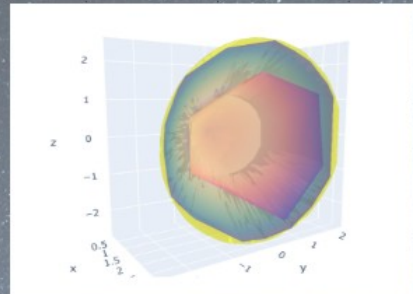
*Thank you!  
Obrigado!  
Grazie!*

# Ejecta's Reflectance and Synthetic Imaging

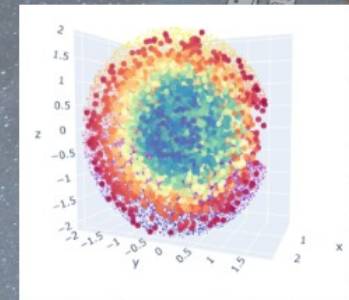
## Schematics



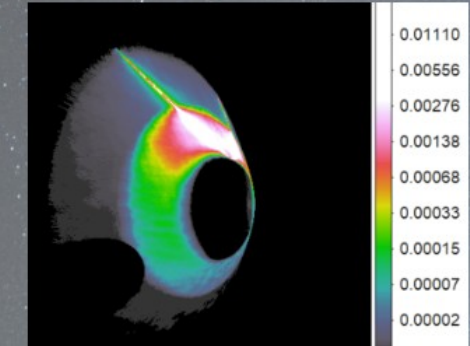
particles evolving through space and time  
Number per population size bins log -5 to -3



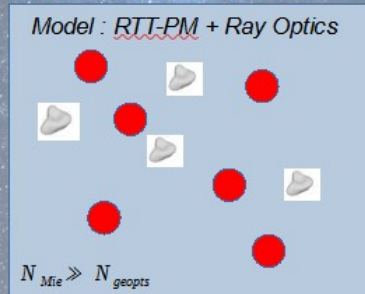
Plume's Convex Hull: incidence, emergence  
And phase angle hitting the cloud's boundaries



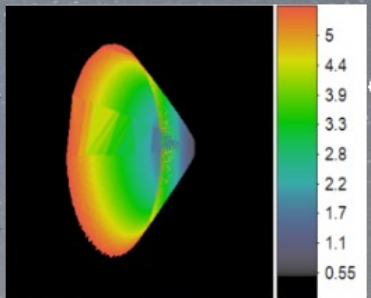
Probability Distribution Function:  
Densities per population per volume



Synthetic Image:  
Optical depth, reflectance and radiance  
Per pixel

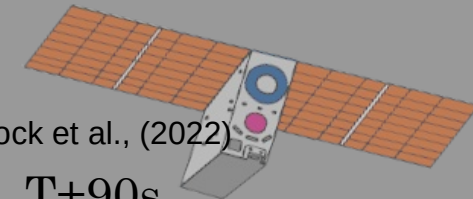


0.5  $\mu$ m <  $\sigma$  < 80  $\mu$ m  
Mishchenko et al ; 2015  
100  $\mu$ m <  $\sigma$  < 3 mm  
Muinonen et al ; 2009



Ray tracing and Scene:  
Columnar pixel densities,  
Geometries, optical depth

# Ejecta's Reflectance and Synthetic Imaging



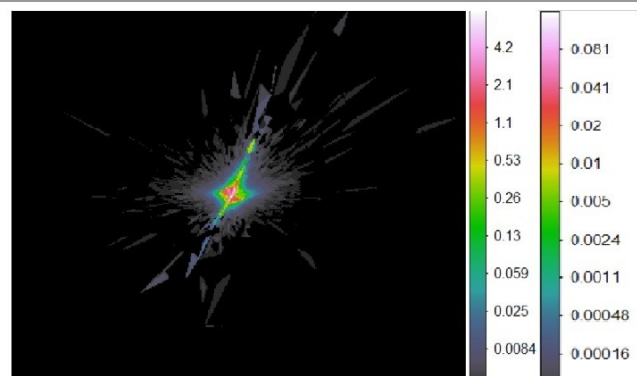
Test with 1M particles, impact input from Fahnestock et al., (2022)

The synthetic images are built over the particle density and coordinate outputs of the particle integrator LICEI (LICIACube Ejecta Integrator, Rossi et al., 2022, PSJ).

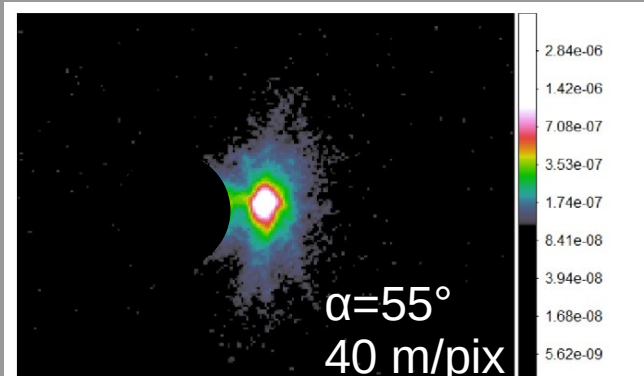
Comparing the resolved ejecta images to synthetic ones help setting constraints to the expansion velocity, grain size distribution, composition, optical depth, and total ejecta mass.

Synthetic imaging also helps discriminating structures that are product of variations in observational conditions and gradients in optical depth.

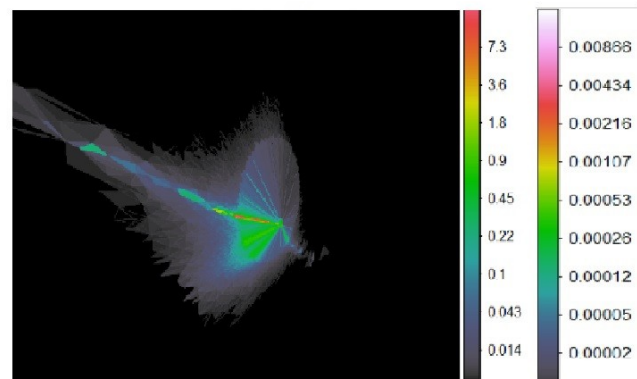
T+90s



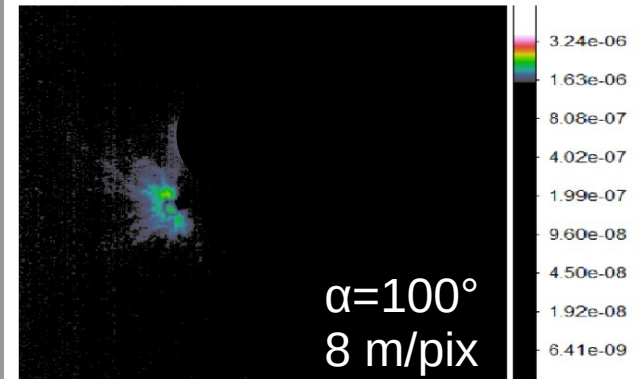
T+90s



T+180s



T+180s



# LICIACube witness DART impact event

